Tensile Strength and Its Variation for PAN-Based Carbon Fibers. II. Calibration of the Variation from Testing

Jiangwei Yao,[1] Weidong Yu[1,2]

[1]*College of Textiles, Donghua University, Shanghai 200051, China*
[2]*Wuhan University of Science and Engineering, Wuhan 430074, China*

Received 22 September 2005; accepted 12 January 2006
DOI 10.1002/app.24455
Published online in Wiley InterScience (www.interscience.wiley.com).

ABSTRACT: The tensile behavior of carbon fibers shows large scattering. This is due to the fiber itself and the testing operations. Because of the high tenacity and modulus, low strain, and easy breakability in bending, not only is the tensile test for single carbon fibers extremely difficult, but the measured results are also oppugned. To achieve a reliable and accurate characterization, several factors influencing the objective and exact testing of single carbon fibers have been measured and discussed, including the wrong pretension, nonaxial stretching, and adhesion effects. The experimental results indicate that the error of strain causing them ranges from 1.5 to 12.3%. Because of the typical linear stress–strain curves of carbon fibers, the ratio of the strain error to the modulus error is approximately equal to 1 : 1, so the calibration of the measured strain must be conducted for the accurate evaluation of the modulus and itself. The calibration is put forward. © 2007 Wiley Periodicals, Inc. J Appl Polym Sci 104: 2625–2632, 2007

Key words: fibers; fracture; mechanical properties

INTRODUCTION

The data measured by a single-carbon-fiber tensile test show a wide variation. Obviously, some of the data scattering, except for the fiber itself, results from the testing methods. In the past 30 years, ASTM D 3379, a standard test method for the tensile strength and Young's modulus of high-modulus, single-filament materials, has been accepted as the way for determining the high-modulus, single-filament strength.[1,2] In fact, the tensile test for brittle and high-tenacity fibers is different from that for flexible fibers. It is difficult to mount a brittle, single fiber on a tensile machine without damage to the fiber and to apply only a tensile load to the fiber. Therefore, a window-card method is suggested in the ASTM D 3379 standard instead of mounting the fiber directly on the tensile machine to avoid any damage to the carbon fibers. However, there are also some errors in the test with the window-card method.

Several studies and discussions have been undertaken in this field. Thomas and Tang[3] verified that the single-filament tensile test is less reliable than the bundle test because of its high coefficient of strength variation. Chi et al.[4] concluded that there are shortcomings in single-filament measurements, such as the difficulty of extracting individual fibers from a bundle and the loss of weaker fibers because they are brittle and easy to fracture in the sampling. Li and Langley[5] proposed a system compliance factor derived from the plotting of the indicated compliance versus the gauge length over the square of the fiber diameter, instead of versus the gauge length alone. Huang et al.[6] also studied an improved method to obtain a more accurate modulus in single-filament measurements.

Much attention should be paid to this kind of experimental operation because of the small size and fragility of the fibers. First, the force to break a single fiber, especially the bending force, is so small that any extra and nonaxial stress introduced during the sampling and testing may result in fiber damage or even fracture, that is, measuring-error magnification and test failure. Second, the elongation to failure for brittle fibers is relatively short, even at a long gauge length, and the fiber modulus is high, so the wrong recording of the elongation to the fiber must occur once there is motion deformation in the initial stretching. Obviously, the two effects will result in low stress, high strain, and low modulus for the fiber being measured.[5] Third, there are various types of damage to the fiber in the sample preparation and testing process, such as picking a fiber up from a bundle, adhering the fiber to a window card, mounting the fiber sample to the tensile machine, and even the chemical action of adhesives on the fiber.

In this work, those factors causing errors, namely, the pretension, adhesive effects, gauge length, and nonaxial stretching, are discussed, and a tensile-curve calibration is put forward.

Correspondence to: W. Yu (wdyu@hdu.edu.cn).

Journal of Applied Polymer Science, Vol. 104, 2625–2632 (2007)

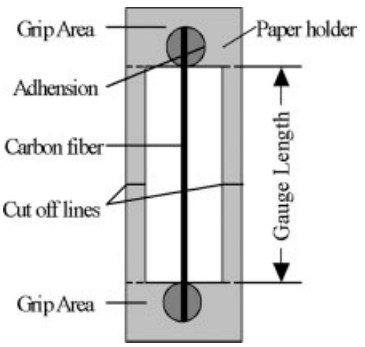

Figure 1 Window card.

EXPERIMENTAL

Carbon fibers

The samples were the same carbon fibers mentioned in part I of this series (7.0-μm average diameter in tows of 12,000 filaments).

Tensile tests

The gauge length adopted for the tensile tests was 40 mm. A fiber randomly selected from the fiber bundle was fixed with an adhesive epoxy resin onto a window tab and aligned along the center axis of the tab, as shown in Figure 1. The length of the fiber between the two adhesive ends was designated the gauge length, which was approximated to the window length, that is, the nominal gauge length (GL_0). After the epoxy resin was cured, the two ends of the tab were grasped between the upper fixed clamp and lower moveable clamp of a tensile tester and then cut off the paper frame. The fiber between the two clamps was extended to failure at the rate of 5 mm/min. The fracture load was measured with a load cell with a capacity of 100 cN.

Diameter measurements

The ASTM D 3379 standard recommends the use of an average cross-sectional area for stress calculation, which is obtained from the measurement of at least 20 fibers in the sample bundle. This may be acceptable for commercial fibers or fibers with comparatively small variations in the fiber diameter. In fact, carbon fibers do exhibit appreciable variation in the cross-sectional area from fiber to fiber. The real stress distribution of carbon fibers cannot be obtained by the division of the force distribution by the mean cross section because of the diameter variation. Therefore, the cross-sectional area evaluated from the fiber average diameter in this study was measured by microscopy for each fiber before the tensile test, and the minimum diameter of each fiber was measured too.

Because the tensile strength of the carbon fibers showed large scattering, about 500 single-filament tests were conducted to analyze the carbon-fiber tensile properties, and the experimental results appeared to be acceptable.

RESULTS AND DISCUSSION

Pretension effect

The bending and tensioning of testing fibers are mainly caused by the wrong pretension. The appropriate state is that, under pretension, the fiber adhering to two joints must be straight but not stretched. For a carbon fiber, the pretension should be zero because the fiber itself is rigid, brittle, and straight. If the pretension is positive and large enough, the window card will be bent, as illustrated in Figure 2; thus, the tested strain will be smaller than the actual strain of the carbon fiber because the gauge length is shorter than the nominal one and there is already elongation at the beginning

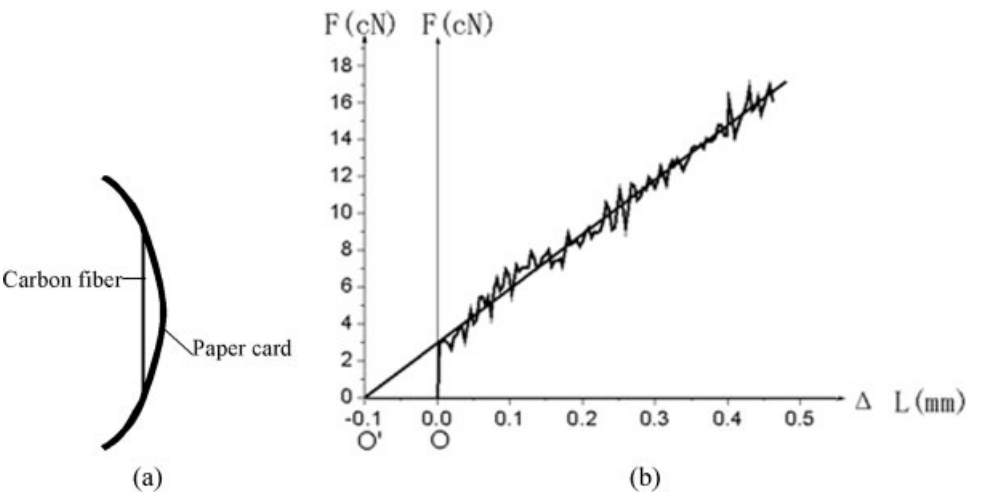

Figure 2 Positive pretension on the carbon fiber and its tensile curve: (a) window-card deformation and (b) force–elongation curve.

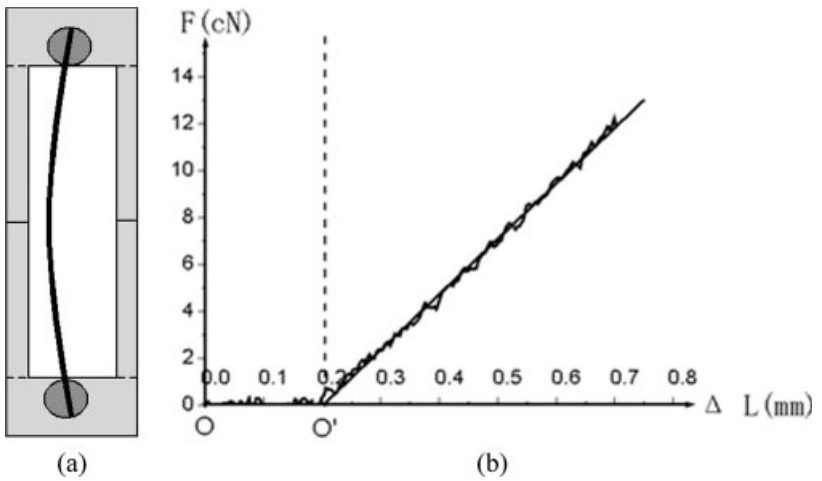

Figure 3 Negative pretension on the carbon fiber and its tensile curve: (a) carbon-fiber bending and (b) force–elongation curve.

because of the tap stretching. If the pretension is negative and strong enough, the fiber between the adhesive joints is bent, as shown in Figure 3, and the tested strain will be larger than the actual strain of the carbon fiber because the stretched fiber length is longer than GL_0. The true elongation originates from O', not from O, to measure the true strain for both the positive and negative pretensions. Only if the true strain is obtained is the modulus calculation of the fiber correct.

To overcome the pretension effect, not only must the sample preparation be careful, but the gauge length must also be calibrated according to the tensile curves, as shown in Figures 2(b) and 3(b). The actual gauge length (GL_p) is

$$GL_p = GL_0 + OO' \quad (1)$$

OO' is directly dependent on the pretension of the carbon fibers. The pretension is related to the sample-made process and the sample-clamped process. It is difficult to limit the pretension within a narrow range. Therefore, it cannot be neglected. The way to calculate the OO' is given in Figure 3. The calibrated results are listed in Table I.

In Table I, σ, ε, and E_0 represent the fracture stress, fracture strain, and modulus of the carbon fibers; CV_σ, CV_ε, and CV_E are the coefficients of variation of the stress, strain, and modulus, respectively. ''Before calibration'' means the tested results were obtained without any calibration. ''After calibration'' means that the tested results were already calibrated.

The difference between the calibrated and uncalibrated test results is listed in Table I as the difference rate:

$$\text{Difference rate} = \frac{(\text{After calibration} - \text{Before calibration})}{\text{After calibration}}$$

OO' may take a relatively high percentage of the actual gauge length because the ratio of OO' to the gauge length varied from -0.96 to 1.75% in these experiments, whereas the OO' value varied from -0.36 to 0.55 mm. The actual strain becomes smaller than the measured value without the calibration of OO'; that is, OO' is not subtracted from the tested strain.

Adhesive effect

Position of the adhesion joints

In the testing operation, the adhesion joints sometimes were away from the set positions, as shown in Figure 4(a); thus, the actual gauge length (GL_{a1}) must be different from the set one. The gauge length should be calibrated by the observation of the position deviations (Δ_1 and Δ_2) of the adhesion joints from the window

TABLE I
Effect of Calibration on the Wrong Pretension

	σ (GPa)	CV_σ (%)	ε (%)	CV_ε (%)	E_0 (GPa)	CV_E (%)
Before calibration	3.39	22.04	1.58	24.86	214.56	19.97
After calibration	3.39	22.04	1.54	21.43	220.13	18.56
Difference rate	0%	0%	−2.60%	−16.01%	2.53%	−7.60%

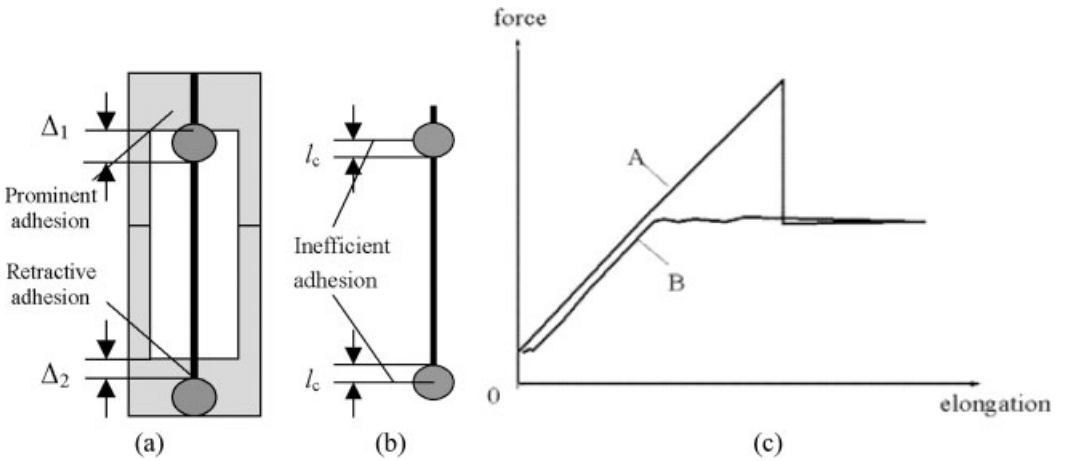

Figure 4 Position and efficiency of the adhesion joints: (a) wrong position of the joints, (b) efficiency of the adhesion joints, (c) and tensile curve of inefficient adhesion.

edge with a microscope while the fiber diameter is measured:

$$GL_{a1} = GL_0 + \Delta_1 + \Delta_2 \quad (2)$$

Δ ($\Delta = \Delta_1 + \Delta_2$) is the most controllable error. The mean value of Δ is very small and far less than 1 mm; the largest value was 0.09 mm in our experiments. Moreover, it is rather tedious to measure it for every sample, so that if the mean value of Δ is less than the actual gauge length divided by 100, it can be neglected because the error of strain caused by Δ is approximately 0.01%.

Efficiency of the adhesion joints

Besides the influence of the position (Δ) of the adhesion joints, the adhesive effect can also cause a change in the gauge length. If GL_0 is the inside length between the two adhesive joints, GL_{a2} will become larger than GL_0 because there is an ineffective length of the adhered fibers, as shown in Figure 4(b), which is like the critical slippage length (l_c) in the pullout test used to evaluate the interfacial shearing stress of carbon fibers. The ineffective adhesion length, which is equal to l_c, depends on the adhesive, so l_c varies with various adhesives.

The interfacial shearing force between the fiber surface and the epoxy resin must be no smaller than the tensile force in the carbon fiber. Otherwise, the fiber will be pulled from the epoxy resin, and the tensile force cannot be obtained. Figure 4(c) shows two tensile curves of carbon fibers that were pulled out instead of being broken. Curve A indicates that the interfacial shear force was less than the tensile fracture force of the carbon fiber, so the interface between the carbon fiber and epoxy resin was broken, but there still was friction between the surface of the carbon fiber and the epoxy resin. Curve B indicates that the interfacial shear force was even less than the friction between the surface of the carbon fiber and the epoxy resin.

According to the classical calculation,[7] l_c can be calculated. Because

$$2\pi r l_c \tau = \pi r^2 \sigma \quad (3)$$

l_c is

$$l_c = r\sigma/2\tau \quad (4)$$

where r is the radius of the carbon fiber, τ is the interfacial shear strength of the carbon fiber, and σ is the tensile strength.

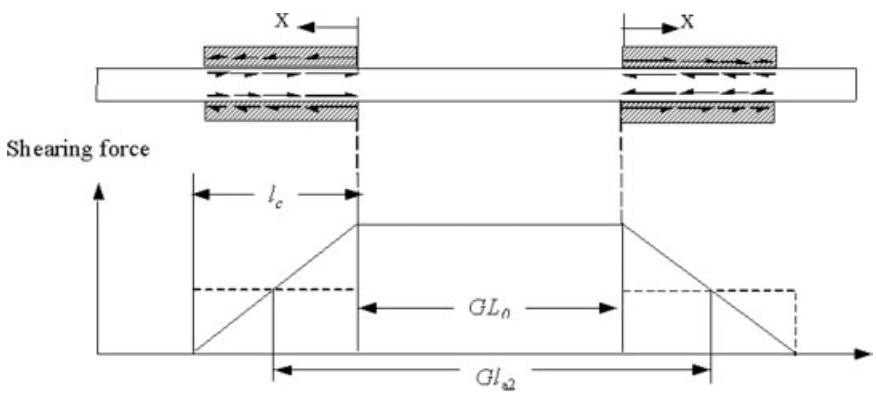

Figure 5 Scheme of the ineffective adhesion length.

TABLE II
Effect of Calibration on the Ineffective Adhesion Length

	σ (GPa)	CV_σ (%)	ε (%)	CV_ε (%)	E_0 (GPa)	CV_E (%)
Before calibration	3.39	22.04	1.54	21.43	220.13	18.56
After calibration	3.39	22.04	1.46	19.52	232.19	19.84
Different rate	0%	0%	−5.48%	−9.78%	−5.19%	6.45%

As we can see in Figure 5, the distribution of the interfacial stress on both of the adhesion ends makes the stretched fiber length, namely, the actual gauge length (GL_{a2}), longer than GL_0. The actual length is the sum of GL_0 and $2l_c$. However, at the l_c section of the fiber, the interfacial shear stress decreases with an increase in the value of x in the l_c section; that is, the strain caused by the shearing stress decreases with x increasing. Consequently, the effective strain at l_c corresponds only to that of $l_c/2$, so the extra gauge length is half of $2l_c$:

$$\Delta l = 2 \times 0.5 \times l_c \qquad GL_{a2} = GL_0 + l_c \tag{5}$$

where Δl is extra gauge length caused by the ''ineffective length'' of the adhered fibers. The question is how to find the exact l_c value, which is an important parameter for the calculation of GL_{a2} because of the obvious volume dependence of carbon fibers,[8] especially for the length dependence.[9] There are two approaches to evaluating the $_c$. The first way is an experiential way in round numbers. l_c, similar to that in the pullout test, can be evaluated by means of the pullout[10] or fragmentation test[11] empirically. Therefore, the previously tested results for l_c (10^{-1} to 10^0 mm[10–12]) can be regarded as the reference of the evaluation. The second method is to follow our measurements because the slippage occurred in this experiment when the length of the adhesion joint was less than 2 mm, as shown in Figure 4(c). This result is close to that of the previous investigation.[13] Therefore, we use our result to estimate the strain error caused by the reason.

The tested results for the tensile properties were calibrated according to the modification and are shown in Table II. The effect of the ineffective adhesion length (i.e., l_c) on the tested strain is about 5.48% in the difference rate and approximates the modulus (5.19%).

According to the aforementioned analysis, if the fiber is parallel to the stretch direction, the real gauge length considering the pretension and adhesion effect is the sum of GL_0, OO', Δ, and l_c.

$$\text{Gauge length} = GL_0 + OO' + \Delta_1 + \Delta_2 + l_c. \tag{6}$$

Just as in the previous Δ discussion, only if l_c is less than the centesimal of GL_0 can it be neglected. Thus, if GL_0 is large enough, the sum of all errors, that is, $OO' + \Delta_1 + \Delta_2 + l_c$, can be neglected.

The influence can be evaluated in total by tests at different gauge lengths, as illustrated in Figure 6. First, we measure the elongations at small GL_0 values (at least <50 mm), and K_1 is determined as the extrapolated value of elongation/GL_0 at the zero gauge length; then, we measure the elongation at high GL_0 values (at least >200 mm), and K_2 is determined as the extrapolated value of elongation/GL_0 at the zero gauge length. The value of $(1/K_1 - 1/K_2)$ stands for the effect of $OO' + \Delta_1 + \Delta_2 + l_c$.

Nonaxial stretching

Various sorts of nonaxial stretching

Because of the experimental operation, not all carbon fibers were parallel to the shifting direction of the

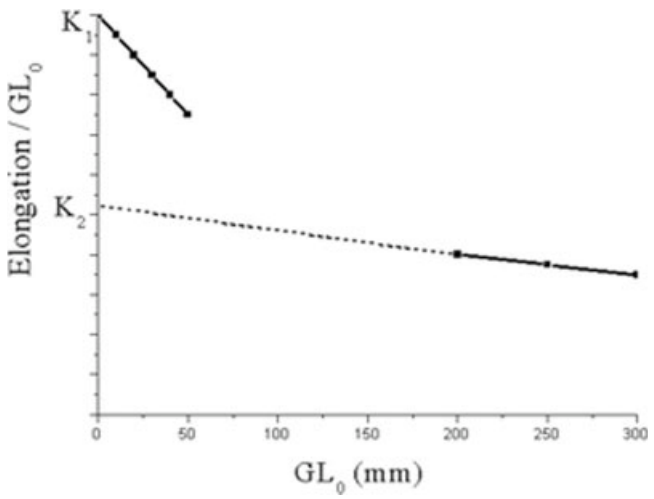

Figure 6 Calibration of the gauge length.

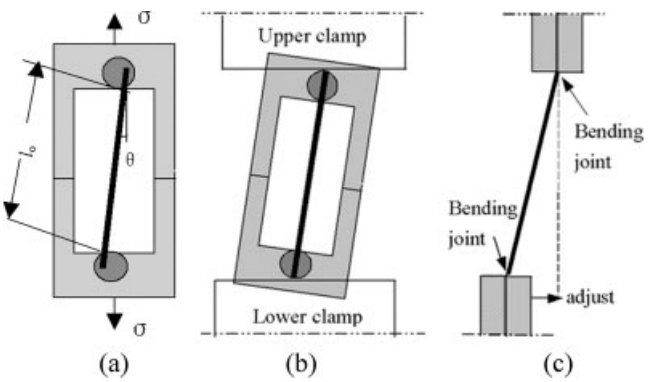

Figure 7 Nonaxial stretching: (a) fiber inclining in the window card, (b) nonaxial clamping, and (c) noncoplanar clamping faces.

TABLE III
End Effect on the Axial Stretching

Sample	σ (GPa)	CV_σ (%)	ε_a (%)	$CV_{\varepsilon a}$ (%)	ε (%)	CV_ε (%)	E_0 (GPa)	CV_E (%)
Axial stretching	3.39	22.04	1.58	24.86	1.46	19.52	232.19	19.84
End effects	3.16	19.84	1.59	24.44	1.40	21.59	225.71	17.85

lower clamps in the monofilament tensile test. A test in which a carbon fiber is not parallel to the clamp-shifting direction is called nonaxial stretching here. The nonaxial stretching may be caused by two incorrect operations. One is the fiber inclining in the window card; that is, the fiber is not parallel to the symmetrical axis of the window card, as shown in Figure 7(a). The other is nonaxial clamping; that is, the central axis of the window card is not parallel to the direction of stretching, as shown in Figure 7(b). In addition, nonaxial stretching will occur if the two clamping faces are not coplanar. Nevertheless, it is not considered here because the error can be adjusted before the test.

Theoretical discussion

When the fiber or window card is gripped in the jaws of a tensile machine not parallel to the direction of stretching, both tested stress and strain values become inaccurate. The reasons are twofold.

First, there is a joint-end effect, that is, bending damage at the bending joints. Some fibers fail because of the stress concentrations at each end of the fiber adjacent to the adhesion joints: there is bending and shearing stress because of angle θ. These are called end effects.

ε and CV_ε in Table III represent the calibrated strain and its coefficient of variation. More nonaxially clamped fibers failed adjacent to the glue spots than those of the axial-stretching sample, and the fiber tensile strength in the end effect was smaller than that of the axial-stretching test. One of the reasons is that the nonaxially clamped fibers were bent and sheared at the adhesion joint. The results of Table IV are proof because the percentage of end breaking increases with an increase in the indicated angle (θ).

Second, the tested strain of nonaxially clamped fibers was larger than that of the axial-stretching sample because the angle between the axes of the window card and the direction of stretching became smaller gradually during the stretch process, corresponding to a low actual strain in the fibers.

TABLE IV
End-Effect Percentage of Nonaxial Stretching

Sample	Axial stretching	7° clamping	10° adhesion	20° adhesion
End breaking (%)	12.43	12.96	14.20	18.12

If the upper clamp is fixed while the lower clamp moves down only in the vertical direction without any horizontal movement

$$\varepsilon_r = \frac{l_1 - l_0}{l_0} \tag{7}$$

$$\varepsilon_a = \frac{h_1 - h_0}{h_0} = \frac{l_1 - l_0}{h_0} = \frac{l_0}{h_0} \cdot \varepsilon_r \tag{8}$$

$$\varepsilon_t = \frac{\Delta e}{e} = \frac{e_1 - e_0}{e_0} \tag{9}$$

where ε_r is the reading strain, ε_a is the tested strain, ε_t is the fiber strain, Δe is the true elongation of the carbon fiber during stretching and e is the actual fiber gauge length. Figure 8 shows that e_1 is equal to h_1 sec θ_1, and e_0 is equal to h_0 sec θ_0. ε_a can be obtained:

$$\frac{\Delta e}{e} = (1 + \varepsilon_a)\left(\frac{\sec\theta_1}{\sec\theta_0}\right) - 1 = (1 + \varepsilon_a)\sqrt{\frac{1 + \tan^2\theta_1}{1 + \tan^2\theta_0}} - 1 \tag{10}$$

Rearranging eq. (10), we find

$$\begin{aligned}\varepsilon_\theta = \frac{\Delta e}{e} &= \sqrt{1 + 2\varepsilon_a \cdot \cos^2\theta_0 + \varepsilon_a{}^2 \cdot \cos^2\theta_0} - 1 \\ &= \sqrt{1 + 2\varepsilon_r \cdot l_0 \cdot \cos^2\theta_0/h_0 + \varepsilon_r{}^2 \cdot l_0{}^2 \cdot \cos^2\theta_0/h_0{}^2} - 1\end{aligned} \tag{11}$$

where ε_θ is the uncalibrated strain when the angle between the fiber axial and the stretching direction is θ.

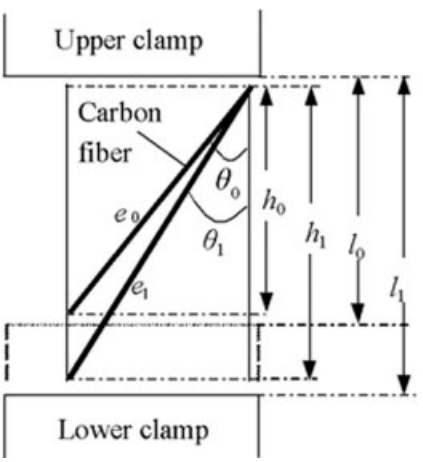

Figure 8 Strain analysis of nonaxial stretched fibers.

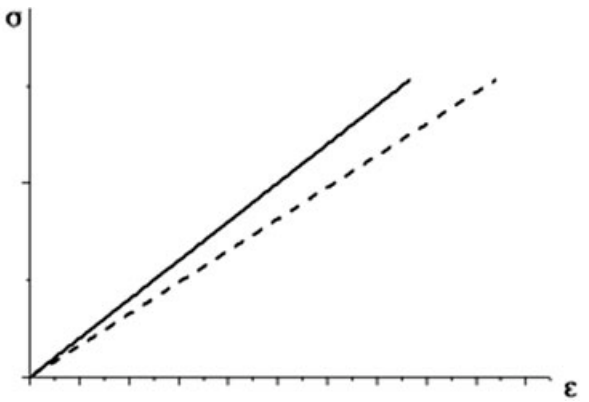

Figure 9 Theoretical σ–ε curves for (—) standard and (- - -) nonaxial stretching.

The true strain is

$$\varepsilon = \frac{\Delta e}{e}\left(1 - \frac{C_S}{\Delta e/F}\right) \tag{12}$$

where C_S is the system compliance factor and F is the stretching force.

If the samples are nonaxially clamped, e_0 is the stretched fiber length. For the fiber inclining in the window card

$$e_0 = \mathrm{GL}_0 \times \sec\theta + OO' + \Delta + l_c$$

$$h_0 = e_0 \times \cos\theta = \mathrm{GL}_0 + (OO' + \Delta + l_c) \times \cos\theta$$

For the nonaxial clamping

$$e_0 = \mathrm{GL}_0 + OO' + \Delta + l_c$$

$$h_0 = e_0 \times \cos\theta = (\mathrm{GL}_0 + OO' + \Delta + l_c) \times \cos\theta$$

For the axial-stretching sample

$$e_0 = h_0 = \mathrm{GL}_0 + OO' + \Delta + l_c$$

as in eq. (6).

If the end effect is not considered and the stress–strain curve of carbon fibers is a linear line, the tensile behavior can be estimated with the theoretical calculation, as illustrated in Figure 9. The solid line is the tensile curve for axial stretching, whereas the dashed line is ε_a [eq. (8)] when θ is 10°. The theoretical σ–ε curve for nonaxial stretching (θ = 10°) is different from axial stretching on its low slope and high strain. Hence, the effect of nonaxial stretching should be considered and calibrated.

The calibrated results obtained from eq. (12) are listed in Table V:

$$\varepsilon_{cs} = \frac{\Delta l}{l}\left(1 - \frac{C_S}{\Delta l/F}\right)$$

$$\Delta\varepsilon = \frac{\text{Calibrated strain value} - \varepsilon_a}{\text{Calibrated strain value}}$$

$$\Delta E = \frac{\text{Calibrated modulus value} - E_a}{\text{Calibrated modulus value}}$$

where l means the true gauge length, C_s is the system compliance as mentioned in ASTM D3379, Δε (ΔE) means the difference rate between the calibrated strain (modulus) and the tested strain (modulus), respectively. ε_{cs} means partly calibrated strain of carbon fibers, the strain error caused by C_s is calibrated while the strain error caused by the angle between the fiber axial and the stretching direction is not calibrated. The calibrated strain (ε) is 2–10% smaller than ε_a and close to the strain obtained from axial stretching (1.46%). The calibrated modulus (E_0) is 2–9% higher than the tested one. The tested stress obtained from nonaxial stretching is 1–19% smaller than that from axial stretching, being dependent on the increased angle and the percentage of end breaking. All these errors are significant and cannot be ignored.

TABLE V
Effect of Calibration on Nonaxial Stretching

Sample	σ (GPa)	CV_σ (%)	ε_a (%)	ε_{cs} (%)	$\Delta\varepsilon_{cs}$ (%)	ε_t (%)	$\Delta\varepsilon_t$ (%)	ε (%)	Δε (%)	CV_ε (%)
Axial stretching	3.39	22.04	1.47	1.46	−0.68	1.46	−0.68	1.46	−0.68	19.52
7° clamping	3.36	13.23	1.46	1.45	−0.69	1.44	−1.39	1.43	−2.10	25.88
10° adhesion	2.95	19.37	1.56	1.55	−0.65	1.53	−1.96	1.51	−3.31	23.32
20° adhesion	2.85	18.79	1.59	1.58	−0.63	1.46	−8.90	1.45	−9.66	27.41

Sample	*Ea* (GPa)	*Ecs* (GPa)	Δ*Ecs* (%)	*Et* (GPa)	Δ*Et* (%)	*E*0 (GPa)	Δ*E*0 (%)	CV*E* (%)
Axial stretching	230.61	232.19	0.68	232.19	0.68	232.19	0.68	19.84
7° clamping	230.14	231.72	0.68	233.33	1.37	234.96	2.05	18.70
10° adhesion	189.10	190.32	0.64	192.81	1.92	195.36	3.20	21.44
20° adhesion	179.25	180.38	0.63	195.21	8.18	196.55	8.80	24.76

$\Delta\varepsilon_{cs}$ ($\Delta\varepsilon_t$) mean the difference rate between the calibrated strain and the ε_{cs} (ε_t), respectively. E_a, E_{cs}, and Et means σ/ε_a, σ/ε_{cs} and σ/ε_t, respectively. ΔE_{cs} (ΔE_t) mean the difference rate between the calibrated strain and the E_{cs} (E_t), respectively. E_0 means the true initial modulus, ΔE_0 means the difference rate between the calibrated modulus and the uncalibrated modulus.

However, the strain error decreases quickly with the reduction of the inclining angle. The error at a small angle of nonaxial stretching (no greater than 4°) can be neglected according to the estimation of eq. (12). To avoid the effect, setting an indicator on clamps is advisable, so we put an indicating wire on the clamp to check and adjust the fiber samples in all tests, except for the purposed setting.

The aforementioned discussion is only for nonaxial stretching without the horizontal movement of clamps, but if there is horizontal movement due to various tensile instruments, the error caused by the effect of the nonaxial stretching can be calibrated similarly. Meanwhile, the end effects and nonaxial stretching effects on the tensile properties is higher in theory than those of both vertical and horizontal shifts of the clamps.

CONCLUSIONS

Because of the low strain value resulting from the brittleness of carbon fibers, the tested strain must be obtained and calibrated to be accurate; otherwise, a significant error of the fiber modulus or even stress occurs. In this experiment, the ratio of the strain error to the modulus error is about 1 : 1 (as listed in Tables I and II), and the modulus value of carbon fibers is often 2.1–2.4 $\times$ 10^2 GPa; this means that the strain error, ranging from 2 to 7%, can cause a modulus error of 4–15 GPa. Therefore, the accurate evaluation and calibration of the actual strain are essential.

The wrong pretension, nonaxial stretching, and adhesion effects all influence the tested strain. The strain error caused by the wrong pretension, about 2.5%, can be taken out accurately by the calibration of the measured tensile curves. The nonaxial stretching effect can be controlled within a small range by careful operation and an indicating wire. If the angle between the fiber and stretched direction is not bigger than 4°, the error caused by the nonaxial stretching can be neglected. Among all factors, the adhesion effect induces the biggest error and is difficult to control and estimate accurately. The experimental results indicate that the ineffective adhesion length, that is, l_c, is about 5.7% of GL_0, the strain error will be about 5.5% of the strain, and the modulus will be about 5.1% lower than the real modulus.

The calibration methods for all these factors are put forward. For the wrong pretension, OO' should be added to the gauge length. From eqs. (11) and (12), the strain error caused by nonaxial stretching can be calibrated. Therefore, there exist two approaches to calibrating the ineffective adhesion, that is, the experiential method and the method shown in Figures 5 and 6.

References

1. Standard Test Method for Tensile Strength and Young's Modulus for High-Modulus Single-Filament Materials; ASTM D 3379-75; American Society for Testing and Materials: West Conshohocken, PA, 1975.
2. Lara-Curzio, E. Ceramic Fibers, Distribution of Fiber Strengths and Continuous Fiber Reinforced Ceramic Matrix Composites. http://www.ornl.gov/~webworks/cpr/pres/108966.pdf (Jan. 24, 2004).
3. Thomas, A. D.; Tang, L. G. Int SAMPE Tech Conf 1999, 31, 26.
4. Chi, Z.; Chou, T. W.; Shen, G. J Mater Sci 1984, 19, 3319.
5. Li, C. T.; Langley, N. R. J Am Ceram Soc C 1985, 68, 202.
6. Huang, J.; Zhang, B.; Zhu, J.; Yang, B.; Xu, S. Presented at the 1st Pacific Rim International Conference on Advanced Materials and Processing, Hangzhou, China, June 1992.
7. Kelly, A.; Tyson, W. R. J Mech Phys Solids 1965, 13, 329.
8. Tetsuy, T.; Takashi, M. Mater Sci Eng A 1997, 238, 336.
9. Moreton, R. Fiber Sci Technol 1969, 1, 273.
10. Zhandarov, S. F.; Pisanova, E. V. Compos Sci Technol 1997, 57, 957.
11. Pittman, C. U.; Jiang, W.; He, G. R.; Gardner, S. D. Carbon 1998, 2, 25.
12. Rashkovan, I. A.; Korabelnikov, Y. G. Compos Sci Technol 1997, 57, 1017.
13. Kettle, A. P.; Beck, A. J.; O'Toole, L.; Jones, F. R.; Short, R. D. Compos Sci Technol 1997, 57, 1023.